European Journal of Radiology 138 (2021) 109674

Contents lists available at ScienceDirect

European Journal of Radiology

journal homepage: www.elsevier.com/locate/ejrad

Research article

Geometric 3D analyses of the foot and ankle using weight-bearing and non weight-bearing cone-beam CT images: The new standard?

M. Broos [a], S. Berardo [b], J.G.G. Dobbe [c], M. Maas [a], G.J. Streekstra [a,c], R.H.H. Wellenberg [a,*]

[a] Department of Radiology and Nuclear Medicine, Amsterdam UMC, Location AMC, Amsterdam Movement Sciences, Amsterdam, the Netherlands
[b] Ospedale Maggiore della Carità di Novara, Istituto di Radiodiagnostica ed Interventistica, Università del Piemonte Orientale, Novara, Italy
[c] Department of Biomedical Engineering and Physics, Amsterdam UMC, Location AMC, Amsterdam, the Netherlands

ARTICLE INFO

Keywords:
Computed tomography
Cone-beam CT
Weight-bearing CT
Geometrical analyses

ABSTRACT

Objectives: We hypothesize that three-dimensional (3D) geometric analyses in weight bearing CT-images of the foot and ankle are more reproducible compared to two-dimensional (2D) analyses. Therefore, we compared 2D and 3D analyses on bones of weight-bearing and non weight-bearing cone-beam CT images of healthy volunteers.
Methods: Twenty healthy volunteers (10 male, 10 female, mean age 37.5 years) underwent weight-bearing and non weight-bearing cone-beam CT imaging of both feet. Clinically relevant height and angle measurements were performed in 2D and 3D (for example: cuboid height, calcaneal pitch, talo-calcaneal angle, Meary's angle, intermetatarsal angle). Three-dimensional measurements were obtained using automated software. Intra-observer and inter-observer agreement were evaluated for all 2D measurements.
Results: Overall intraclass correlation coefficients (ICC's) were higher than 0.750 for most 2D measurements, ranging from 0.352 to 0.995. Calcaneal pitch, angle between the first metatarsal (MT1) and proximal phalange 1, between the fifth metatarsal (MT5) and the calcaneus and heights of the sesamoid bones, navicular, cuboid and talus decreased during weight-bearing in both 2D and 3D results ($p < 0.01$). Meary's angle was not statistically different in 2D ($p = 0.627$) and 3D ($p = 0.765$). Higher coefficients of variation in 2D geometric analysis parameters (0.27 versus 0.16) indicate that 3D analyses are more precise compared to 2D ($p < 0.01$). Results of left and right feet are comparable for 2D and 3D analyses.
Conclusion: Although 2D and 3D geometrical analyses are fundamentally different, automated 3D analyses are more reproducible and precise compared to 2D analyses. In addition, 3D evaluation better demonstrates differences in bone configurations between weight-bearing and non weight-bearing conditions, which may be of value to demonstrate pathology.

1. Introduction

Conventional CT and radiography help clinicians recognize and locate problems in the foot and ankle. To assess pathological foot morphology, weight-bearing radiography is often used in standard care in patients with Charcot foot, diabetic foot or neuropathic foot, where severe deformities of the foot result in a change of anatomy and response of inter-bone alignment as a result of loading [1–3]. However, the 2D nature of radiography limits the evaluation of morphological changes due to the complex three-dimensional (3D) structure of the foot and ankle. Also, over-projection of bones in both anterior-posterior and lateral views may affect the reliability of quantitative and qualitative analyses [1]. Furthermore, disorders with accompanying deformities may only be visible under natural loading, since the accompanying load likely alters the configuration of the bones in the foot.

In a weight-bearing cone-beam CT (CBCT) scanner, 3D images of the lower extremities can be acquired with natural loading and without load in the upright position. This type of functional imaging may reveal problems that would otherwise be non-discernible [4–8], such as the displacement and rotation of bone fragments in patients with

Abbreviations: Ax, axial; C, calcaneus; CBCT, cone-beam computed tomography; CP, calcaneal pitch; CV, coefficient of variation; ICC, intraclass correlation coefficient; IMA, intermetatarsal angle; MT1, first metatarsal; MT2, second metatarsal; MT5, fifth metatarsal; Non WB, non weight-bearing; P1, first phalange; P2, second phalange; Sag, sagittal; SD, standard deviation; T, talus; TC, talocalcaneal angle; WB, weight-bearing.

* Corresponding author.
E-mail addresses: m.broos@asz.nl (M. Broos), sara.berardo@maggioreosp.novara.it (S. Berardo), j.g.dobbe@amsterdamumc.nl (J.G.G. Dobbe), m.maas@amsterdamumc.nl (M. Maas), g.j.streekstra@amsterdamumc.nl (G.J. Streekstra), r.h.wellenberg@amsterdamumc.nl (R.H.H. Wellenberg).

https://doi.org/10.1016/j.ejrad.2021.109674
Received 28 December 2020; Received in revised form 13 March 2021; Accepted 18 March 2021
Available online 20 March 2021

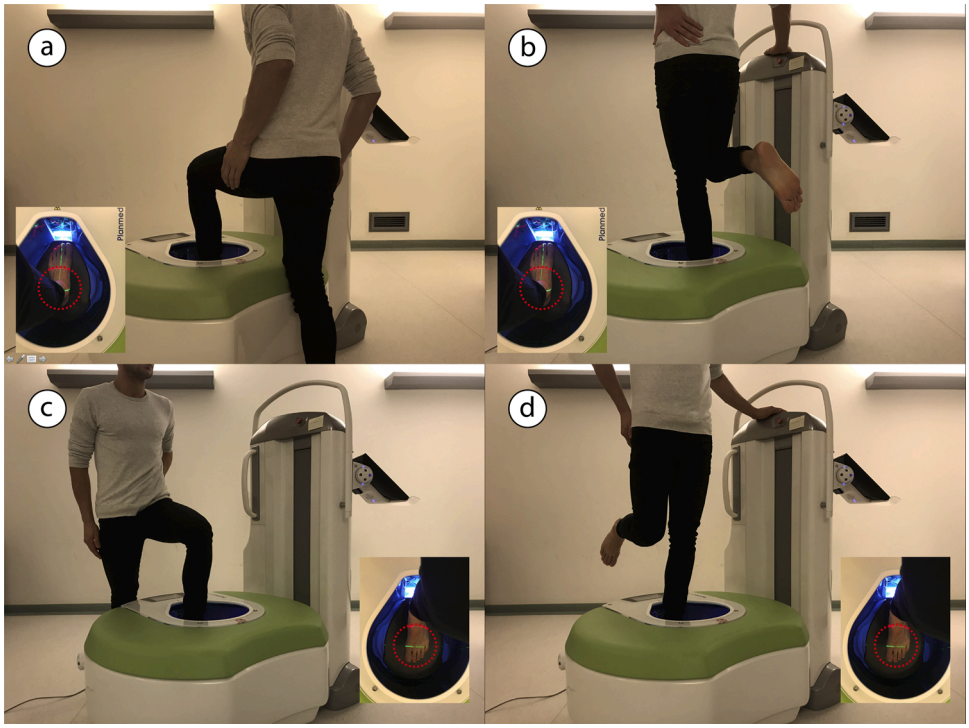

Fig. 1. Weight-bearing and non weight-bearing cone-beam CT images were acquired under natural load. For both feet the hindfoot is acquired in non weight-bearing (a) and weight-bearing (b). Also the forefoot of both feet was acquired in non weight-bearing (c) and weight-bearing condition (d).

deformities and a diminished joint space in patients with osteoarthritis [9,10]. Studies in forefoot and hindfoot alignment show that 3D weight-bearing CT is more useful than 2D imaging, since 3D volume data allows for a better multi-planar insight [3,11–13]. However, the added value of utilizing geometrical parameters measured in 3D instead of 2D equivalents is unclear. In daily surgical practice, the contralateral side is often used as reference in corrective surgery [14–16], although the symmetry is only confirmed from 2D radiographs [17] but not in 3D space. In could be of practical value if geometrical 2D or 3D parameters of the contralateral foot could serve as reference in diagnosis and corrective surgery. However, the validity of using the contralateral side as geometrical reference in correction surgery of the ankle and foot disorders is unknown. Therefore we propose to evaluate geometrical parameters extracted from 3D weight-bearing and non weight-bearing images as well as 2D radiogram equivalents extracted from 3D volume data, which enables a fair 2D versus 3D comparison [2,12].; The objectives of this study were to compare 2D with 3D geometrical parameters, compare these parameters in weightbearing and non weight-bearing conditions, and between the left and right feet. In addition, we evaluated the inter-and intra-observer variability in 2D and 3D geometric parameters. To this end, we evaluated 2D and 3D images of healthy volunteers.;

2. Materials and methods

2.1. Subjects

In this pilot study 20 healthy volunteers with no history of foot and ankle pathology were included. The group consisted of ten men and ten women with a mean age of 37.5 years (ranging between 24–57 years, SD = 9.9 years). Volunteers had a mean weight of 75.6 kg (ranging between 53 and 108 kg, SD=13.9 kg). The average height was 177.2 cm (ranging between 154−191 cm, SD = 9.5 cm). Medical ethical approval was obtained (METC2019_038). Exclusion criteria were inability to stand on one leg, aged under 18, pregnancy or no written informed consent.

2.2. Acquisition

Non weight-bearing and single-leg-full-weight-bearing images were acquired on a Planmed Verity cone-beam CT system (Planmed Oy) (Fig. 1). This system uses cone beam CT (CBCT) technology to provide 3D images of the extremities at a particularly low dose similar to several repeated plain radiographs [18]. Patients stand in the upright position in the weight-bearing CT scanner, with a field-of-view of approximately 16 × 13 cm [19]. Scan parameters were: 96 kV and 6.3 mA and a pulse length of 20 ms. Five hundred projection images were used to reconstruct 3D images with a voxel size of 0.2 × 0.2 × 0.2 mm. Due to field-of-view limitations, hindfoot and forefoot images were acquired separately. In each patient, weight-bearing and non weight-bearing images of the left and right hindfoot and forefoot were acquired, resulting in 8 acquisitions in total, resulting in a total CTDI of 48.64 mGy and DLP of 634.16 mGy*cm. Consecutive images of the hindfoot and forefoot were stitched together using stitching software (Planmed Oy).

2.3. Bone segmentation

Before 3D measurements could be obtained, different osseous structures in the feet were segmented (by **) using Articulus software [20]: distal tibia and fibula, talus, calcaneus, os naviculare, os cuboideum, os cuneiforme medial/intermedius/lateral, 1st metatarsal (MT1), 2nd metatarsal (MT2), 5th metatarsal (MT5), 1st and 2nd proximal phalange and the sesamoid bones. Segmentation of bones was performed in non weight-bearing scans by region-growing with manual editing, and was followed by level-set segmentation and extraction of a polygon mesh representing the bone [20]. Repositioning of bones in weight-bearing conditions was determined by registration. The bones which were segmented in the non weight-bearing CT scan were manually positioned in the correct weight-bearing position and orientation. The software optimizes the position and orientation of the bones in weight-bearing conditions via translation and rotation based on local intensities and bone-soft tissue transitions. The average time spend for bone segmentation and registration was approximately 6 h per healthy

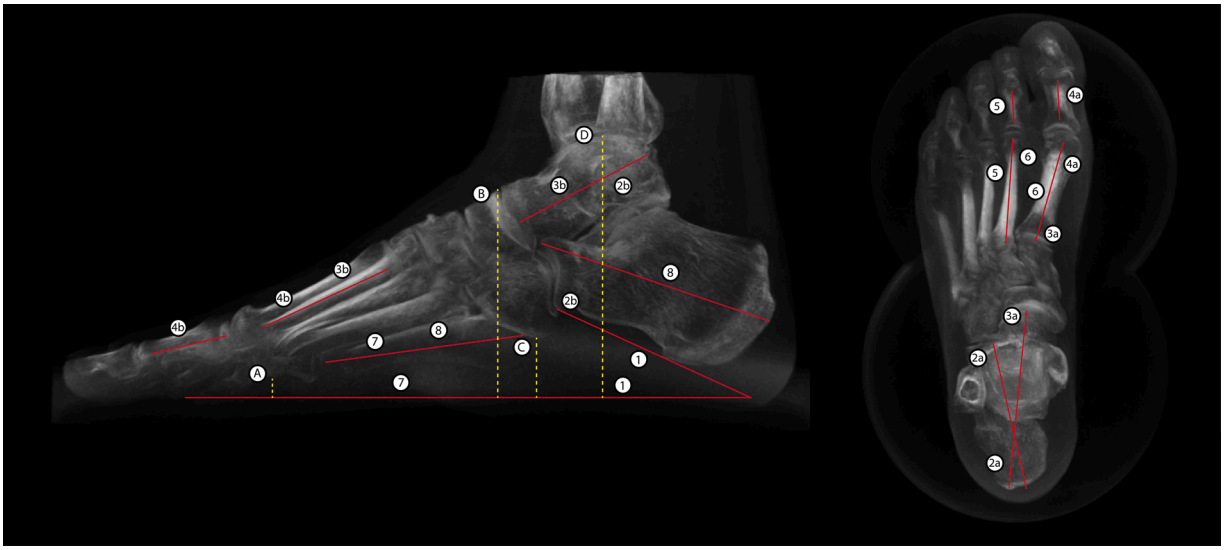

Fig. 2. Digitally reconstructed radiographs of the foot in lateral view (left) and craniocaudal view (right), showing lines drawn by an investigator, which are used to perform 2D measurements (see text). Angles are defined by two lines with the same number. Heights are defined by the length of lines indicated by a letter.

volunteer, including WB and non WB data of both feet.

2.4. Measurements - 2D

Two-dimensional simulated X-ray images were extracted from weight-bearing and non weight-bearing images in fixed sagittal and axial views (by **) using the Digitally Reconstructed Radiograph (DRR) function in HOROS software (version 3.3.6). These simulated X-rays were used for geometrical measurements on the foot anatomy. In literature, several well-known angle and height measurements are described to determine the stability of the foot and ankle [4,21–26]. Angles between bones were defined by manually drawn anatomical axis lines through the center of the body structures in 2D sagittal and/or axial view of the foot (Fig. 2). The angles evaluated were: calcaneal pitch (1), talo-calcaneal angle axial (2a) and sagittal (2b), angle between the talus and MT1 axial (3a) and sagittal/Meary's angle (3b), angle between MT1 and proximal phalange axial (4a) and sagittal (4b), angle between MT2 and proximal phalange 2 sagittal (5), intermetatarsal angle sagittal (6), angle between MT5 and the ground sagittal (7), angle between MT5 and the calcaneus sagittal (8). Heights are defined by the length of lines indicated by a letter and were measured from the horizontal surface until the most caudal or cranial part of the bone structure (Fig. 2). The heights evaluated were those of the sesamoid bones of MT1 (A), navicular (B), cuboid (C) and talus (D). HOROS was also used for these 2D measurements. All measurements were performed by two blinded observers (** and **) to test the inter-observer variability, and were repeated by one of the observers (**) to test the intra-observer variability

2.5. Measurements - 3D

Articulus software was used to obtain all 3D measurements. By using the bone structures in weight-bearing and non weight-bearing positions, the software automatically composes anatomical long-axes of the bone structures based on their inertial axes [27]. The following measurements were obtained (by **) in 3D: calcaneal pitch (1), talo-calcaneal angle

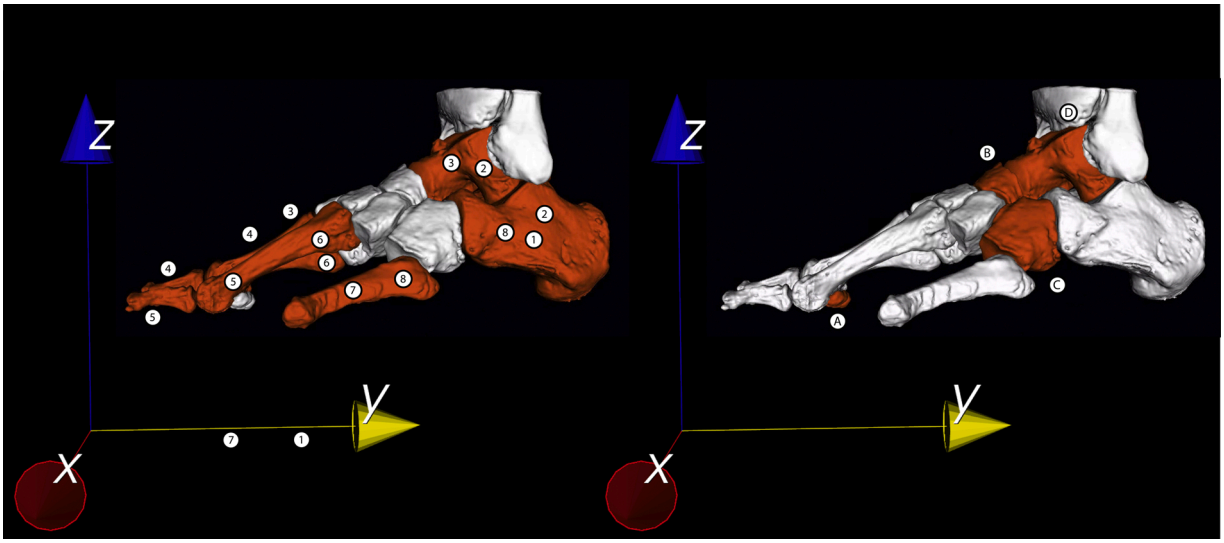

Fig. 3. Segmented 3D osseous structures in Articulus with X, Y, Z-axes. The numbers and letters indicate angles and heights, which are specified in the text. Angles are defined using the long-axis of bones with the same number. Heights were measured from the most caudal or cranial point of the mesh with respect to the scanners axes.

Table 1
Overview of the mean, standard deviation (SD), median and 95 % confidence interval (CI) and the coefficient of variation (CV) of 2D weight-bearing (WB) and non weight-bearing (NWB) measurements. Differences between WB and NWB results (NWB-WB) and p-values are provided.

		Left feet								Right feet							
2D measurements		NWB Mean	Median (95 % CI)	CV	WB Mean	Median (95 %CI)	CV	Mean difference NWB-WB	P value	NWB Mean	Median (95 % CI)	CV	WB Mean	Median (95 %CI)	CV	Mean difference NWB-WB	P value
1	Calcaneal pitch (sag) (°)	24.55	24.24 (22.21−26.89)	0.20	22.68	21.69 (20.24−25.11)	0.23	−1.88	<0.001*	25.17	24.21 (22.80−27.54)	0.20	23.61	23.41 (21.32−25.91)	0.21	−1.56	<0.001*
2a	Talo-calcaneal angle (ax) (°)	18.32	18.06 (17.36−19.27)	0.11	18.90	18.21 (17.83−19.98)	0.12	0.59	0.073	18.96	18.82 (17.91−20.01)	0.12	19.08	19.02 (14.09−20.06)	0.11	0.12	0.654
2b	Talo-calcaneal angle (sag) (°)	46.97	47.05 (44.57−49.37)	0.11	46.67	46.80 (44.49−48.86)	0.10	−0.30	0.97	47.27	48.74 (44.94−49.60)	0.11	46.66	47.26 (44.56−48.77)	0.10	−0.61	0.006*
3a	Angle talus-MT1 (ax) (°)	5.82	5.29 (4.27−7.36)	0.57	5.51	4.44 (3.69−7.34)	0.71	−0.30	0.627	5.27	4.56 (3.50−7.04)	0.72	4.46	3.75 (3.12−5.76)	0.64	−0.82	0.247
3b	Angle talus-MT1 (sag) (°)	5.31	5.92 (4.15−6.47)	0.47	4.93	4.79 (3.89−5.98)	0.45	−0.38	0.627	5.31	5.16 (4.21−6.41)	0.44	4.34	4.43 (3.44−5.24)	0.44	−0.97	0.03*
4a	MT1 prox phal 1 (ax) (°)	15.43	13.85 (12.88−17.99)	0.35	14.40	13.90 (11.68−17.12)	0.40	−1.03	0.046*	13.98	13.39 (12.26−15.69)	0.26	13.19	12.80 (11.46−14.92)	0.28	−0.78	0.108
4b	MT1 - prox phal 1 (sag) (°)	13.60	13.66 (10.85−16.36)	0.43	11.24	11.33 (8.75−13.73)	0.47	−2.36	<0.001*	12.64	11.97 (10.16−15.11)	0.42	10.72	10.29 (8.57−12.87)	0.43	−1.91	0.001*
5	MT2 prox phal 2 (ax) (°)	5.65	6.68 (4.39−6.91)	0.48	4.43	4.68 (3.25−5.61)	0.57	−1.22	0.019*	4.56	3.99 (3.12−6.00)	0.67	3.81	3.18 (2.73−4.89)	0.61	−0.75	0.079
6	Intermetatarsal angle (ax) (°)	9.72	9.59 (8.71−10.74)	0.22	10.28	10.31 (9.26−11.30)	0.21	0.56	0.065	10.16	10.31 (9.60−10.71)	0.12	11.01	10.75 (10.10−11.91)	0.18	0.85	0.021*
7	MT5 - ground (sag) (°)	10.53	10.08 (9.59−11.46)	0.19	9.18	8.74 (8.27−10.10)	0.21	−1.34	<0.001*	11.08	10.88 (9.94−12.22)	0.22	9.54	9.29 (8.58−10.51)	0.22	−1.54	<0.001*
8	MT5 - calcaneus (sag) (°)	29.70	29.99 (27.51−31.90)	0.16	27.27	27.47 (25.05−29.50)	0.17	−2.43	<0.001*	30.05	29.8 (27.70−32.39)	0.17	27.75	28.04 (25.58−29.91)	0.17	−2.30	<0.001*
A	Fat pad caput MT1 (sag) (mm)	7.95	7.02 (6.57−9.34)	0.37	6.04	5.45 (5.10−6.98)	0.33	−0.19	0.001*	7.60	7.6 (6.43−8.77)	0.33	6.47	6.41 (5.35−7.58)	0.37	−0.11	0.001*
B	Navicular height (sag) (cm)	7.21	7.33 (6.89−7.53)	0.09	6.81	6.87 (6.51−7.11)	0.09	−0.40	<0.001*	7.24	7.33 (6.96−7.52)	0.08	6.91	7.12 (6.60−7.22)	0.10	−0.33	<0.001*
C	Cuboid height (sag) (cm)	2.37	2.39 (2.20−2.54)	0.15	2.24	2.19 (1.98−2.51)	0.25	−0.13	0.002*	2.34	2.32 (2.19−2.49)	0.14	2.12	2.09 (1.96−2.29)	0.17	−0.22	<0.001*
D	Talar height (sag) (cm)	8.85	8.99 (8.51−9.20)	0.08	8.54	8.54 (8.21−8.87)	0.08	−0.32	<0.001*	8.94	9 (8.62−9.25)	0.08	8.60	8.65 (8.26−8.93)	0.08	−0.34	<0.001*

NWB: non weight-bearing.
WB: weight-bearing.
CV: coefficient of variation.
CI: confidence interval.
* Statistically significant difference.

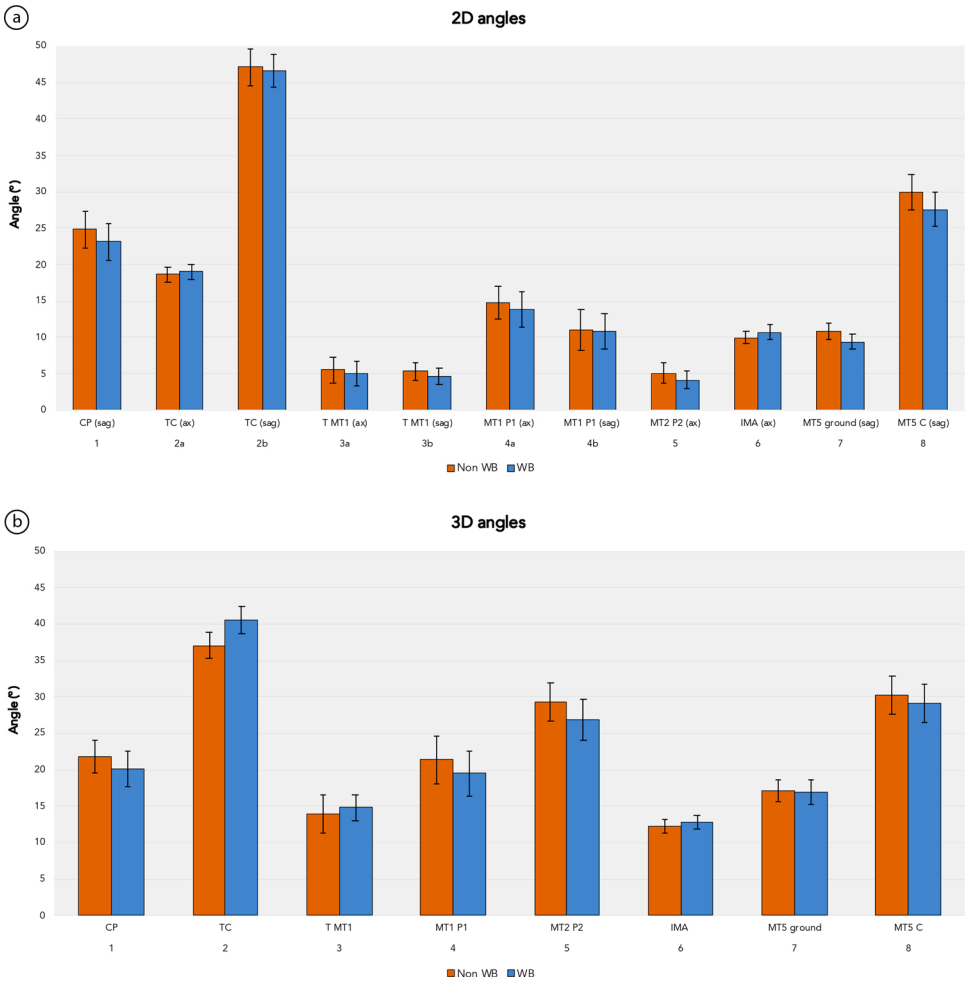

Fig. 4. Mean 2D angles (a) and 3D angles (b) with standard deviations measured in non weight-bearing (non WB) and weight-bearing (WB) conditions.
Ax: axial.
Sag: sagittal.
Non WB: non weight-bearing.
WB: weight-bearing.
CP: calcaneal pitch.
TC: talocalcaneal angle.
T: talus.
MT1: first metatarsal.
MT2: second metatarsal.
P1: first phalange.
P2: second phalange.
IMA: intermetatarsal angle.
MT5: fifth metatarsal.
C: calcaneus.

(2), angle between the talus and MT1 / Meary's angle (3), angle between MT1 and proximal phalange (4), angle between MT2 and proximal phalange 2 (5), intermetatarsal angle (6), angle between MT5 and the ground (7), the angle between MT5 and the calcaneus (8), caudal height of the sesamoid bones (E), cranial height of the navicular bone (F), caudal height of the cuboid bone (G) and cranial height of the talus (H). The caudal and cranial height of the sesamoid bones, navicular, cuboid and talus were not measured with respect to the surface, on which the volunteers were standing on, but were measured from the most caudal or cranial point of the mesh with respect to the scanners reference plane. In case of the calcaneal pitch and the angle of MT5 with respect to the ground, a reference Y-axis was created equal to the ground (Fig. 3).

2.6. Statistical analyses

Analysis of inter- and intra-observer reliability was done by determining the intra-class correlation coefficient (ICC) between the different observers. An ICC value higher than 0.750 was considered a good reliability, where an ICC value higher than 0.900 was considered an excellent reliability [28]. Shapiro-Wilk test was used to determine if results were normally distributed. All 2D measurements of both observers and 3D measurements were averaged per measurement parameter. Mean, standard deviation (SD), median and 95 % confidence interval (CI) of 2D and 3D weight-bearing (WB) and non weight-bearing (non WB) geometrical analyses were calculated. Coefficient of variation was calculated to determine the precision of 2D and 3D measurements. Weight-bearing results were subtracted from non weight-bearing results (non WB-WB) in order to calculate mean differences between WB and non WB results. A negative result represents a decrease in angle or height during weight-bearing. Mean differences between weight-bearing and non weight-bearing, between 2D and 3D measurements and between left and right comparisons were evaluated using the Wilcoxon-signed rank test. Wilcoxon-signed rank test was used since not all data was normally distributed and a relatively small sample size of >25 was used. SPSS software (version 25, IBM) was used, a significance level of 5% was used for all tests and tests were two-tailed.

3. Results

3.1. 2D measurements

The agreement of 2D measurements between and within observers was good to excellent in most cases. The average ICC for all measurements was 0.861 and ranged from 0.352 to 0.995. Low ICC exceptions were mainly found in angle measurements involving the talus, calcaneus and MT1. For example the ICC of Meary's angle was 0.360 for the right foot without load and 0.579 for the talo-calcaneal angle (sagittal) of the left and right feet without load and 0.352 for the talo-calcaneal angle (axial) of the right feet with load. All other measurements showed an ICC value of at least 0.750 or higher.

Geometrical parameters in weight-bearing images were significantly different compared to non weight-bearing analysis in the vast majority of the measurements, with mainly smaller angles and decreased heights during weight-bearing (Table 1, Figs. 4a, 5 a). For example, mean calcaneal pitch decreased from 24.6° to 22.7° ($p < 0.001$) and 25.2° to 23.6° ($p < 0.001$) and cuboid height decreased from 2.37 to 2.24 cm

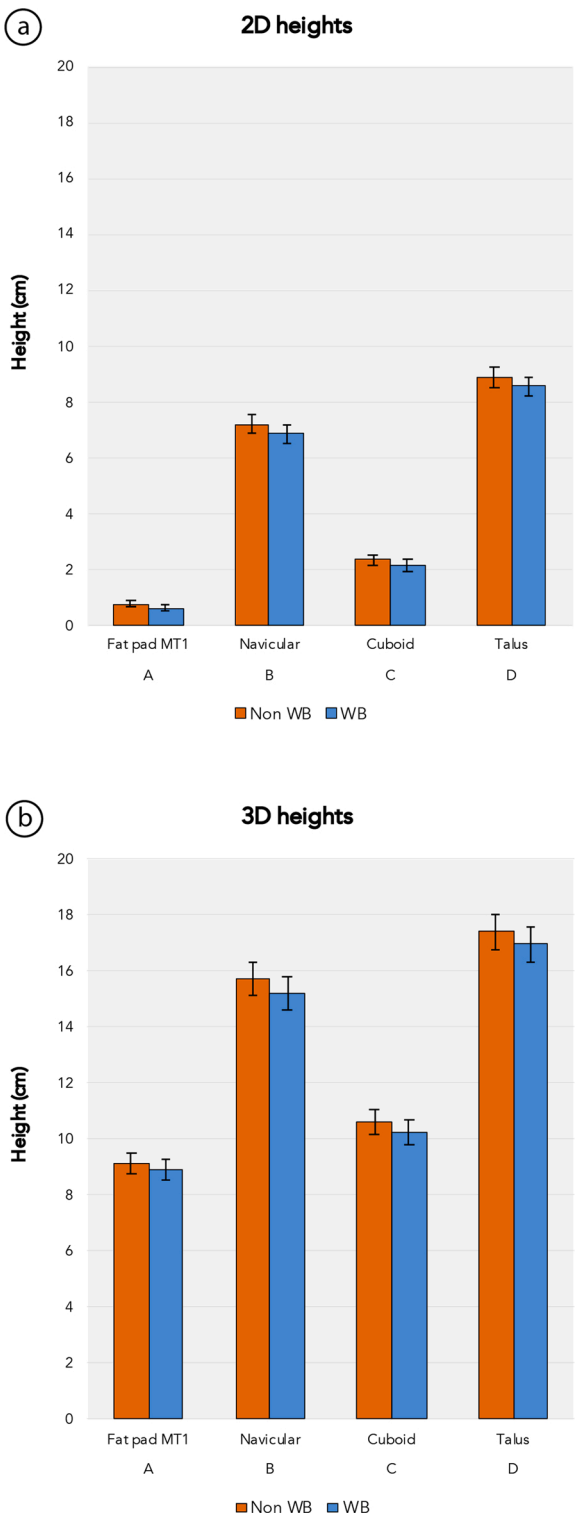

Fig. 5. Mean 2D heights (a) and 3D heights (b) with standard deviations measured in non weight-bearing (non WB) and weight-bearing WB) conditions.
Non WB: non weight-bearing.
WB: weight-bearing.
MT1: first metatarsal.

($p = 0.002$) and 2.34 to 2.12 cm ($p < 0.001$) for the left and right feet respectively. Also, angles between MT1 and the proximal phalange 1 in the sagittal view, between MT5 and the ground and between MT5 and the calcaneus decreased ($p < 0.005$). All bone heights decreased during weight-bearing ($p < 0.005$) (Fig. 5a). No statistical difference was seen in the talo-calcaneal angle (axial) and angle between the talus and MT1 (axial) for both left and right feet results. In some cases, such there was a statistical difference in only the left or right feet measurements. Mean intermetatarsal angle (axial) and talo-calcaneal angle (axial) did not increase or decrease during weight-bearing.

3.2. 3D measurements

During weight-bearing a decrease was observed in calcaneal pitch, angle between MT1 and the proximal phalange 1, angle between MT2 and the proximal phalange 2, angle between MT5 and the calcaneus and heights of the sesamoid, navicular, cuboid and talus (Table 2, Figs. 4b, 5 b). The talo-calcaneal angle and intermetatarsal angle increased during weight-bearing ($p < 0.005$). The angle between MT5 and the ground decreased for the left feet ($p = 0.003$) and increased for the right feet ($p = 0.007$). Meary's angle was not statistically different between non weight-bearing and weight-bearing results.

3.3. Differences between 2D and 3D measurements

Calcaneal pitch, angle between MT1 and proximal phalange 1, between MT5 and the calcaneus and heights of the sesamoid bones, navicular, cuboid and talus decreased in both 2D and 3D results. Differences in angles and heights between non weight-bearing and weight-bearing were small and ranged between several degrees or millimeters in 2D and 3D results. In many parameters the range of values is fundamentally different in 3D compared to 2D.

The coefficient of variation (CV) was calculated to determine the precision of 2D and 3D measurements (Tables 1 and 2). Mean CV of 2D measurements was 0.27 and was significantly higher compared to the mean CV of 3D measurements, which was only 0.16 ($p < 0.01$). There is no significant difference in CV between WB – non WB results and left – right results.

3.4. Differences between geometric parameters of left and right feet

In general, results of left and right feet were comparable for both non weight-bearing and weight-bearing 2D and 3D results. Most of the mean differences between left and right feet were not statistically different for 2D measurements (28/30) and 3D measurements (20/24), except the non weight-bearing results of the talo-calcaneal angle (axial) ($p < 0.05$) and angle between MT2 and the proximal phalange 2 ($p < 0.05$) in 2D and the calcaneal pitch ($p < 0.05$) and angle between MT5 and the ground ($p < 0.001$) in 3D.

4. Discussion

In this study we compared 2D and 3D geometric parameters of the foot and ankle by analyzing weight-bearing and non weight-bearing cone-beam CT images of the left and right feet of twenty healthy volunteers. We demonstrated that the coefficient of variation in 3D parameters was generally lower than in 2D parameters, which indicates that 3D parameters are a more precise representation of the geometric parameters. We found a significant difference between many 2D geometric parameters between non WB and WB. However, as a result of the lower variability of 3D parameters, we found that all 3D geometric parameters, except Meary's angle, were significantly different between non WB and WB parameters. In addition, geometrical results of left and right feet are generally similar for both 2D and 3D analyses.

The 3D geometric parameters in this study, although inspired by the 2D counterparts, are different in nature. The 2D equivalent is often a projection into a single plane in 3D space. The 2D and 3D parameters values are therefore related but not the same. Due to the automatic nature of our 3D assessment, the inter- and intra-observer variabilities were zero. The use of registration furthermore reduced segmentation inaccuracies. For 2D measurements on the other hand the ICC's ranged

Table 2
Overview of the mean, standard deviation (SD), median and 95 % confidence interval (CI) and the coefficient of variation (CV) of 3D weight-bearing (WB) and non weight-bearing (NWB) measurements. Differences between WB and NWB results (NWB-WB) and p-values are provided.

		Left feet								Right feet							
3D measurements		NWB Mean	Median (95 % CI)	CV	WB Mean	Median (95 %CI)	CV	Mean difference NWB-WB	P value	NWB Mean	Median (95 % CI)	CV	WB Mean	Median (95 %CI)	CV	Mean difference NWB-WB	P value
1	Calcaneal Pitch (°)	20.77	20.74 (18.47−23.06)	0.24	19.44	20.03 (16.93−21.96)	0.28	−1.32	<0.001*	22.81	22.57 (20.89−24.74)	0.18	20.92	21.27 (18.88−22.96)	0.21	−1.89	<0.001*
2	Talo-calcaneal angle (°)	36.87	37.28 (35.29−38.45)	0.09	40.69	40.36 (38.99−42.38)	0.09	3.82	<0.001*	37.23	38.51 (35.58−38.88)	0.09	40.36	41.06 (38.48−42.25)	0.10	3.13	<0.001*
3	Angle talus-MT1 (°)	14.26	13.92 (11.81−16.71)	0.37	14.83	14.92 (13.12−16.53)	0.25	0.57	0.765	13.64	14.39 (11.12−16.15)	0.39	14.78	15.05 (13.12−16.45)	0.24	1.14	0.55
4	MT1 - prox phal 1 (°)	21.97	23.32 (18.49−25.46)	0.34	20.21	20.85 (16.89−23.53)	0.35	−1.76	0.002*	20.77	19.03 (18.10−23.45)	0.28	18.77	17.63 (16.24−21.30)	0.29	−2.00	0.005*
5	MT2 - prox phal 2 (°)	29.28	29.28 (26.97−31.59)	0.17	27.34	27.16 (24.68−30.00)	0.21	−1.94	0.021*	29.32	28.61 (26.86−31.79)	0.18	26.35	25.98 (23.77−28.94)	0.21	−2.97	<0.001*
6	Intermetatarsal angle (°)	12.37	12.79 (11.32−13.42)	0.18	12.87	12.55 (12.01−13.74)	0.14	0.5	0.004*	12.12	12.01 (11.27−12.97)	0.15	12.69	12.21 (11.85−13.53)	0.14	0.57	0.001*
7	MT5 - ground (°)	14.57	14.03 (13.30−15.84)	0.19	13.59	13.31 (12.24−14.94)	0.21	−1.05	0.003*	19.57	19.47 (18.06−21.08)	0.17	20.25	19.24 (18.60−21.91)	0.17	0.68	0.007*
8	MT5 - calcaneus (°)	29.96	30.88 (27.38−32.55)	0.18	28.61	29.31 (26.00−31.22)	0.19	−1.35	<0.001*	30.48	30.53 (28.03−32.94)	0.17	29.49	29.74 (27.14−31.83)	0.17	−1.00	0.003*
A	Fat pad caput MT1 (cm)	9.18	9.11 (8.82−9.55)	0.08	8.86	8.88 (8.50−9.23)	0.09	−0.32	<0.001*	9.14	9.20 (8.81−9.47)	0.08	8.93	8.91 (8.56−9.29)	0.09	−0.22	0.001*
B	Navicular height (cm)	15.70	15.63 (15.14−16.26)	0.08	15.14	15.05 (14.61−15.68)	0.08	−0.56	<0.001*	15.72	16.00 (15.20−16.24)	0.07	15.27	15.53 (14.72−15.81)	0.08	−0.45	<0.001*
C	Cuboid height (cm)	10.67	10.60 (10.24−11.09)	0.09	10.26	10.34 (9.86−10.66)	0.08	−0.41	<0.001*	10.60	10.54 (10.21−10.99)	0.08	10.27	10.30 (9.84−10.69)	0.09	−0.33	0.001*
D	Talar height (cm)	17.40	17.49 (16.77−18.03)	0.08	16.91	16.88 (16.31−17.51)	0.08	−0.49	<0.001*	17.38	17.57 (16.81−17.94)	0.07	17.00	17.00 (16.41−17.59)	0.07	−0.38	<0.001*

NWB: non weight-bearing.
WB: weight-bearing.
CV: coefficient of variation.
CI: confidence interval.
* Statistically significant difference.

from 0.352 to 0.992, which is similar to results of Shelton et al. [26]. Low ICC's were most likely caused by over-projection in case of the first metatarsal bone (MT1) and difficulties determining the anatomical long-axis of bones, such as the talus and calcaneus. Our 2D geometric parameters were in agreement with those of other studies reporting parameters of healthy individuals [17,21,23,24,29,30]. Regarding the comparison of geometric parameters for left and right feet our results are in agreement with Tomas et al. who found no significant difference between left and right in AP and LL weight-bearing radiographs [17]. The similarity of the 2D and 3D parameters between the left and right foot suggest that the contralateral side could serve as a reference in corrective surgery. Future research is need to investigate whether the contralateral side is indeed a good reference from a clinical point of view.

Regarding 2D angles, the calcaneal pitch, angle between MT1 and the proximal phalange 1 in the sagittal view, angle between MT5 and the ground and between MT5 and the calcaneus decreased during weight-bearing. In 3D, all weight-bearing results, except from Meary's angle, were statistically different compared to non weight-bearing results. All 3D angles decreased, except from the talo-calcaneal angle, which increased during weight-bearing since the foot moves to valgus position. The bone heights of the sesamoid bones, navicular, cuboid and talus decreased during weight-bearing in both 2D and 3D results due to increase loading of the foot and ankle, thereby decreasing the arches of the foot. We found a higher mean cuboid height (22 mm) compared to Cesar de Netto and Gwani, which can be explained by the fact that both studies included flatfoot patients [11,31]. Since in 3D measurement the software does not correct for the height of the weight-bearing CT platform, a one-on-one comparison with 2D height measurements could not be made. The trends seen in the height differences between weight bearing and non weight bearing conditions were equal in 3D and 2D.

In this study we used simulated radiographs extracted from non WB and WB cone-beam CT scans, with a lower image quality and resolution compared to conventional radiographs, which may be considered a limitation. However, the geometric comparison between 2D and 3D was inherently more reliable than by comparing separately acquired 2D and 3D images, since both 2D and 3D images were obtained from the same acquisition. Another limitation could have been caused by bending of the platform that supports the foot in the weight-bearing condition. This effect might have slightly influenced our findings, although bending of the platform was quantified to be up to only 2−3 mm. Segmentation inaccuracies were not evaluated in this study. However, we investigated this earlier as reported by Eijnatten et al. who found geometric accuracies of, on average, 0.6 mm in case of global thresholding [32]. The segmentation process will improve in our case since we used thin 0.4 mm slices. Moreover, our threshold-connected region growing algorithm is followed by an automatic level-set segmentation growth algorithm, which grows the segmented region to the boundary of the bone [20], which further reduces the observer variability. It is furthermore unlikely that small variations in the shape of the bone models will affect height measurements and axes of gravitation thus angle measurements. Due to the limited field-of-view of 16 × 13 cm, an entire foot was acquired in two separate acquisitions, which were stitched afterwards to a single image. Stitching may have introduced translation errors up to 3 mm and angulation error up to 3° [33]. Also, the extensive post-processing time, which is mainly caused by the manual segmentation of bones, needs to be decreased, e.g. by using machine-learning algorithms, in order to make functional 3D analysis widely applicable in clinical practice. Finally, weight-bearing images were acquired by placing the scanned foot into the weight-bearing CT scanner with full weight on that foot, meanwhile the contralateral foot was lifted from the ground. We are aware that this is not a normal posture, since standing on one foot instead of both feet decreases bone heights and may affect for example Meary's angle and the talo-calcaneal angle due to pronation of the foot. During the last years CBCT gained popularity in extremity imaging, however CBCT is not a standard imaging modality in all hospitals. The systems are relatively cheap, mobile and enable the acquisition of high-resolution images at reduced dose compare to conventional CT. CBCT has proven its added value in patients with musculoskeletal disorders of the foot, ankle, lower leg and knee, especially when the evaluation of images under natural load may provide additional clinical information.

In most studies, specific measurements are obtained using 2D anterior-posterior and lateral-lateral radiographs, where data of 3D angle and height measurements is usually lacking. Three-dimensional weight-bearing imaging and analyses may be of value in diagnosing the severity of flatfoot or hindfoot deformity [3,11,12], tibio-fibular syndesmosis [34–36], and possibly many more patient groups with musculoskeletal disorders. Three-dimensional evaluation furthermore enables the evaluation of translations and rotations in 6 degrees of freedom. In our opinion, evaluating absolute values and differences between geometrical parameters in WB and non WB conditions may be of added valuable to detect pathology and to determine its severity. For future research we recommend investigating possible differences between males and females and investigating the value of comparing geometric parameters between non WB and WB images, and comparing these with the healthy contralateral side in a group of patients with unilateral disorders. Results of this study may provide baseline values, which can be used in future research in various patient groups.

5. Conclusion

In this study we showed that 3D geometric parameter values are fundamentally different, but more reproducible and precise compared to their 2D equivalent. We furthermore demonstrated that results of left and right feet are similar for both 2D and 3D measurements. In addition, 3D evaluation better demonstrates differences in bone configurations between weight-bearing and non weight-bearing conditions, which may be of value to demonstrate pathology.

CRediT authorship contribution statement

M. Broos: Validation, Formal analysis, Investigation, Data curation, Writing - original draft, Visualization. **S. Berardo:** Formal analysis, Investigation, Writing - original draft, Visualization. **J.G.G. Dobbe:** Conceptualization, Software, Validation, Data curation, Writing - original draft, Writing - review & editing. **M. Maas:** Conceptualization, Resources, Writing - review & editing, Supervision, Project administration, Funding acquisition. **G.J. Streekstra:** Conceptualization, Validation, Writing - review & editing, Supervision, Funding acquisition. **R. H.H. Wellenberg:** Conceptualization, Validation, Investigation, Data curation, Writing - original draft, Writing - review & editing, Visualization, Supervision, Project administration, Funding acquisition.

Declaration of Competing Interest

MB No conflicts of interest to disclose. SB No conflicts of interest to disclose. JGG No conflicts of interest to disclose. MM No conflicts of interest to disclose. GJS No conflicts of interest to disclose. RHHW No conflicts of interest to disclose.

Acknowledgement

This research was supported by the Amsterdam Movement Sciences (AMS) research institute.

References

[1] Z.B. Cheung, M.S. Myerson, J. Tracey, E. Vulcano, Weightbearing CT scan assessment of foot alignment in patients with hallux rigidus, Foot Ankle Int. 39 (2018) 67–74, https://doi.org/10.1177/1071100717732549.

[2] J.Z. Zhang, A. Bernasconi, S. Zhang, 3D biometrics for hindfoot alignment using weightbearing computed tomography, Foot Ankle Int. 60 (2019) 720–726, https://doi.org/10.1177/1071100719835492.

[3] A. Burssens, J.P.M. Peiffer, R.M.T. Lenaerts, W. Isg, G.V.J. Victor, Reliability and correlation analysis of computed methods to convert conventional 2D radiological hindfoot measurements to a 3D setting using weightbearing CT, Int. J. Comput. Assist. Radiol. Surg. 13 (2018) 1999–2008, https://doi.org/10.1007/s11548-018-1727-5.

[4] A. Barg, T. Bailey, M. Richter, C. de Cesar Netto, F. Lintz, A. Burssens, et al., Weightbearing computed tomography of the foot and ankle: emerging technology topical review, Foot Ankle Int. 39 (2018) 376–386, https://doi.org/10.1177/1071100717740330.

[5] J.A. Carrino, A. Al Muhit, W. Zbijewski, G.K. Thawait, J.W. Stayman, N. Packard, et al., Dedicated cone-beam CT system for extremity imaging, Radiology 270 (2014) 816–824, https://doi.org/10.1148/radiol.13130225.

[6] E.K.J. Tuominen, J. Kankare, S.K. Koskinen, K.T. Mattila, Weight-bearing CT imaging of the lower extremity, Am. J. Roentgenol. 200 (2013) 146–148, https://doi.org/10.2214/AJR.12.8481.

[7] T. Kimura, M. Kubota, T. Taguchi, N. Suzuki, A. Hattori, K. Marumo, Evaluation of first-ray mobility in patients with hallux valgus using weight-bearing CT and a 3-D analysis system a comparison with normal feet, J. Bone Jt. Surg. Am. 99 (2017) 247–255, https://doi.org/10.2106/JBJS.16.00542.

[8] A. Hirschmann, C.W.A. Pfirrmann, G. Klammer, N. Espinosa, F.M. Buck, Upright Cone CT of the hindfoot: comparison of the non-weight-bearing with the upright weight-bearing position, Eur. Radiol. 24 (2014) 553–558, https://doi.org/10.1007/s00330-013-3028-2.

[9] N.A. Segal, J. Bergin, A. Kern, C. Findlay, D.D. Anderson, Test–retest reliability of tibiofemoral joint space width measurements made using a low-dose standing CT scanner, Skeletal Radiol. 46 (2017) 217–222, https://doi.org/10.1007/s00256-016-2539-8.

[10] N.A. Segal, E. Frick, J. Duryea, M.C. Nevitt, J. Niu, J.C. Torner, et al., Comparison of tibiofemoral joint space width measurements from standing CT and fixed flexion radiography, J. Orthop. Res. 35 (2017) 1388–1395, https://doi.org/10.1002/jor.23387.

[11] C. de Cesar Netto, L.C. Schon, G.K. Thawait, L.F. da Fonseca, A. Chinanuvathana, W.B. Zbijewski, et al., Flexible adult acquired flatfoot deformity, J. Bone Jt. Surg. Am. 99 (2017) 1–12, https://doi.org/10.2106/JBJS.16.01366.

[12] A. Burssens, H. Vermue, A. Barg, N. Krähenbühl, J. Victor, K. Buedts, Templating of syndesmotic ankle lesions by use of 3D analysis in Weightbearing and nonweightbearing CT, Foot Ankle Int. 39 (2018) 1487–1496, https://doi.org/10.1177/1071100718791834.

[13] B. Campbell, M.C. Miller, L. Williams, S.F. Conti, Pilot study of a 3-Dimensional method for analysis of pronation of the first metatarsal of hallux Valgus patients, Foot Ankle Int. 39 (2018) 1449–1456, https://doi.org/10.1177/1071100718793391.

[14] T. Murase, K. Oka, H. Moritomo, A. Goto, H. Yoshikawa, K. Sugamoto, Three-dimensional corrective osteotomy of malunited fractures of the upper extremity with use of a computer simulation system, J. Bone Jt. Surg. Ser. A 90 (2008) 2375–2389, https://doi.org/10.2106/JBJS.G.01299.

[15] P. Schenk, L. Vlachopoulos, A. Hingsammer, S.F. Fucentese, P. Fürnstahl, Is the contralateral tibia a reliable template for reconstruction: a three-dimensional anatomy cadaveric study, Knee Surg. Sports Traumatol. Arthrosc. 26 (2018) 2324–2331, https://doi.org/10.1007/s00167-016-4378-5.

[16] G.R. Yu, X. Yu, Surgical management of calcaneal malunion, J. Orthop. Trauma Rehabil. 17 (2013) 2–8, https://doi.org/10.1016/j.jotr.2012.04.001.

[17] J.L. Thomas, M.W. Kunkel, R. Lopez, D. Sparks, Radiographic values of the adult foot in a standardized population, J. Foot Ankle Surg. 45 (2006) 3–12, https://doi.org/10.1053/j.jfas.2005.10.014.

[18] J. Koivisto, T. Kiljunen, N. Kadesjö, X.Q. Shi, J. Wolff, Effective radiation dose of a MSCT, two CBCT and one conventional radiography device in the ankle region, J. Foot Ankle Res. 8 (2015), https://doi.org/10.1186/s13047-015-0067-8.

[19] S.K. Koskinen, V.V. Haapamäki, J. Salo, N.C. Lindfors, M. Kortesniemi, L. Seppälä, et al., CT arthrography of the wrist using a novel, mobile, dedicated extremity cone-beam CT (CBCT), Skeletal Radiol. 42 (2013) 649–657, https://doi.org/10.1007/s00256-012-1516-0.

[20] J.G.G. Dobbe, M.G.A. de Roo, J.C. Visschers, S.D. Strackee, G.J. Streekstra, Evaluation of a quantitative method for carpal motion analysis using clinical 3D and 4D CT protocols, IEEE Trans. Med. Imaging 38 (2019) 1048–1057, https://doi.org/10.1109/TMI.2018.2877503.

[21] S. Waldt, K. Woertler, Measurements and Classifications in Musculoskeletal Radiology, 1st editio, 2014. Thieme.

[22] D.V. Flores, C. Mejía Gómez, M. Fernández Hernando, M.A. Davis, M.N. Pathria, Adult acquired flatfoot deformity : anatomy, biomechanics, staging, and imaging findings, Radiographics 39 (2019) 1437–1460, https://doi.org/10.1148/rg.2019190046.

[23] C. Carrara, P. Caravaggi, C. Belvedere, A. Leardini, Radiographic angular measurements of the foot and ankle in weight-bearing: a literature review, Foot Ankle Surg. 26 (2020) 509–517, https://doi.org/10.1016/j.fas.2019.07.008.

[24] B.M. Lamm, P.A. Stasko, M.G. Gesheff, A. Bhave, The journal of foot & ankle surgery normal foot and ankle radiographic angles, measurements, and reference points, J. Foot Ankle Surg. 55 (2016) 991–998, https://doi.org/10.1053/j.jfas.2016.05.005.

[25] A. Leardini, D.P.S. Durante, C. Belvedere, P. Caravaggi, C. Carrara, M.L. Berti, et al., Weight-bearing CT technology in musculoskeletal pathologies of the lower limbs: techniques, initial applications, and preliminary combinations with gait-analysis measurements at the Istituto Ortopedico Rizzoli, Semin. Musculoskelet. Radiol. 23 (2019) 643–656, https://doi.org/10.1055/s-0039-1697939.

[26] T.J. Shelton, E.B. Robinson, L. Nardo, E. Escobedo, L. Jackson, C.D. Kreulen, The influence of percentage weight-bearing on foot radiographs, Foot Ankle Spec. 12 (2019) 363–369, https://doi.org/10.1177/1938640018810412.

[27] M.G.A. de Roo, M. Muurling, J.G.G. Dobbe, M.E. Brinkhorst, G.J. Streekstra, S. D. Strackee, A four-dimensional-CT study of in vivo scapholunate rotation axes: possible implications for scapholunate ligament reconstruction, J. Hand Surg. Eur. 44 (2019) 479–487, https://doi.org/10.1177/1753193419830924.

[28] T.K. Koo, M.Y. Li, A guideline of selecting and reporting intraclass correlation coefficients for reliability research, J. Chiropr. Med. 15 (2016) 155–163, https://doi.org/10.1016/j.jcm.2016.02.012.

[29] Y. Lin, J.N. Mhuircheartaigh, J. Lamb, J.W. Kung, C.M. Yablon, J.S. Wu, et al., Imaging of adult flatfoot : correlation of radiographic, AJR Am. J. Roentgenol. 204 (2015) 354–359, https://doi.org/10.2214/AJR.14.12645.

[30] A. Bryant, P. Tinley, K. Singer, A comparison of radiographic measurements in normal, Hallux Valgus, and hallux limitus feet, J. Foot Ankle Surg. 39 (2000) 39–43, https://doi.org/10.1016/S1067-2516(00)80062-9.

[31] A.S. Gwani, M.A. Asari, Z.I.M. Ismail, How the three arches of the foot intercorrelate, Folia Morphol. (Warsz) 76 (2017) 682–688, https://doi.org/10.5603/FM.a2017.0049.

[32] M. van Eijnatten, R. van Dijk, J. Dobbe, G. Streekstra, J. Koivisto, J. Wolff, CT image segmentation methods for bone used in medical additive manufacturing, Med. Eng. Phys. 51 (2018) 6–16, https://doi.org/10.1016/j.medengphy.2017.10.008.

[33] R.H.H. Wellenberg, J.G.G. Dobbe, J. Erkkila, M. Maas, G.J. Streekstra, Marker-less assessment of the geometric error of fused cone-beam CT images of the foot constructed using stitching software, Acta Radiol. 0 (2020) 1–8, https://doi.org/10.1177/0284185120963955.

[34] S. Patel, K. Malhotra, N.P. Cullen, D. Singh, A.J. Goldberg, M.J. Welck, Defining reference values for the normal tibiofibular syndesmosis in adults using weight-bearing CT, Bone Jt. J. 101 (2019) 348–352, https://doi.org/10.1302/0301-620X.101B2.BJJ-2018-0829.R1.

[35] D. Shakoor, G.M. Osgood, M. Brehler, W.B. Zbijewski, C.D.C. Netto, B. Shafiq, et al., Cone-beam CT measurements of distal tibio-fibular syndesmosis in asymptomatic uninjured ankles: does weight-bearing matter? Skeletal Radiol. 48 (2019) 583–594, https://doi.org/10.1007/s00256-018-3074-6.

[36] M.C. Lawlor, M.A. Kluczynski, J.M. Marzo, Weight-bearing cone-beam CT scan assessment of stability of supination external rotation ankle fractures in a cadaver model, Foot Ankle Int. 39 (2018) 850–857, https://doi.org/10.1177/1071100718761035.